Actinide Chemistry

DOI: 10.1002/ange.200501931

How Can Uranium Ions (U^+, U^{2+}) Activate the O–H Bond of Water in the Gas Phase?**

Maria del Carmen Michelini, Nino Russo, and Emilia Sicilia*

Theoretical and experimental investigations of transition metal cations in the gas phase have attracted considerable attention, focusing mainly on the fundamental understanding of activation of prototypical bonds (e.g. C–H, N–H, O–H).[1] Most of these studies dealt with cations of the first and second transition metal rows. However, the heavier 5f-block elements are also of great interest, mainly because of their

[*] Dr. M. d. C. Michelini, Prof. N. Russo, Prof. E. Sicilia
Dipartimento di Chimica
Università della Calabria
Via P. Bucci, Cubo 14C, 87030 Arcavacata di Rende (Italy)
Fax: (+39) 0984-493-390
E-mail: nrusso@unical.it

[**] Financial support from the Università degli Studi della Calabria and MIUR is gratefully acknowledged.

Supporting information for this article is available on the WWW under http://www.angewandte.org or from the author.

unique ability to activate notoriously unreactive molecules such as CH_4 and CO_2.[2] In addition, there is an increasing interest in studying the gas-phase chemistry of actinides in order to obtain a better understanding of the particular character of the electronic structures and energetics of the early actinides, and especially the direct and indirect roles of the 5f electrons in their chemistry.[3] Moreover, the chemistry of uranium, particularly the hydrolysis reaction, is of fundamental importance.[4]

In a recent experimental study,[5] the pathways and rate constants of the reaction of gas-phase uranium cations with H_2O were investigated using a quadrupole ion-trap mass spectrometer (QIT-MS). In the case of the reaction between U^+ and H_2O the reaction products shown in Equations (1) and (2) were detected.

$$U^+ + H_2O \rightarrow UO^+ + H_2 \quad (1)$$

$$U^+ + H_2O \rightarrow UOH^+ + H \quad (2)$$

There is some disagreement in experimental data regarding the relative rates for reactions (1) and (2). In low-energy ion-beam experiments,[6] both reactions were shown to be exothermic with a branching ratio of about 10:1 in favor of the first one. Therefore, it was concluded that the formation of UO^+ is thermodynamically favored at low kinetic energies and the second reaction channel competes only at higher kinetic energies. In the QIT-MS experiments,[5] the minor product UOH^+ was also detected with a branching ratio close to 10:1, in agreement with the ion-beam experiments. In Fourier transform ion cyclotron mass spectrometry (FTICR-MS) experiments, on the other hand,[7,8] reaction (2) was not observed. UOH^+ was formed only under conditions where thermalization was not effective.[8]

The reaction of U^{2+} led to similar products, although reliable reaction rate constants were not determined for this reaction.[5] In contrast, recent experimental data (FTICR-MS) indicate that U^{2+} reacts with H_2O to produce only UOH^{2+}.[9]

We used three approaches of density functional theory (DFT) to analyze the reactions under study (see the Supporting Information for the method chosen and for computational details). First, B3LYP formulation was used together with the Stuttgart/Bonn (SDD) relativistic effective core potential (RECP, small core). The 6-311^{++}G(d,p) basis set of Pople and co-workers was employed for the rest of the atoms (B3LYP/SDD, hereafter, where SDD = Stuttgart/Bonn relativistic effective core potential). Second, the same RECP and basis sets were used together with the PW91 functionals for the exchange and correlation parts of the generalized gradient approximation (PW91/SDD). Additional calculations were performed by using the zero-order regular approximation together with the PW91 functionals (exchange and correlation) and the type TZ2P basis set as implemented in the ADF package (PW91/ZORA). Finally, we analyzed the effect of spin–orbit interaction by performing single-point calculations on the optimized geometries obtained at the PW91/ZORA level within the spin–orbit ZORA approximation (PW91/SO-ZORA).

In both reaction paths, more than one spin state was considered: for U^+ the quartet state (electronic configuration of the outer shells: $5f^37s^2$), which corresponds to the ground state (GS) of the bare cation, and the low-lying sextet ($5f^36d^17s^1$ and $5f^47s^1$) and doublet states ($5f^37s^2$); for U^{2+} the triplet and quintet (GS of the bare cation) states (the electronic configuration is $5f^4$ in both cases).

In Figure 1 we present the reaction pathway for the interaction of U^+ and H_2O.[10] Only in the case of the B3LYP/SDD approximation was possible to correctly determine the U^+ GS. As a consequence, the potential energy profiles were constructed based on the energy results obtained at that level of theory. The quartet state remained the GS for the whole reaction path. Therefore, we restrict our discussion of the $U^+ + H_2O$ reaction pathway to the results for this state.

The first step of the reaction involves the exothermic formation of a stable ion–dipole complex (**I**, Figure 2). The next step, that is, the O–H bond breaking, takes place through

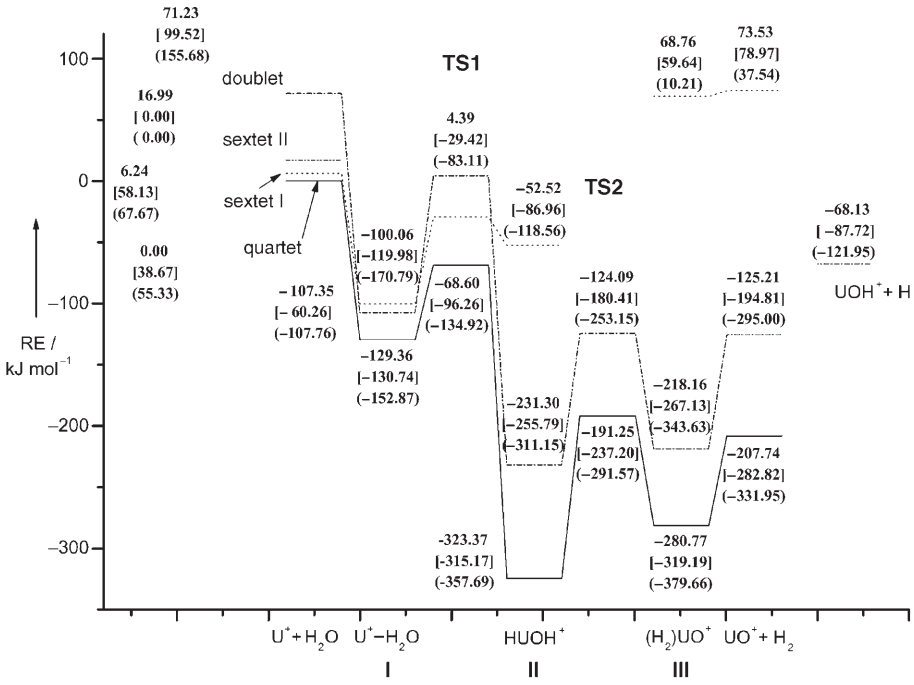

Figure 1. Potential energy profiles (RE: relative energy, in kJ mol^{-1}) for the reaction of U^+ with H_2O at the B3LYP/SDD, PW91/SDD (in square brackets), and PW91/ZORA (in parentheses) levels for the quartet (——), sextet (•••••, –·····), and doublet states (–•–•) of U^+.[10] The statistically averaged experimental data indicate the $5f^37s^2$ configuration (quartet) as the GS of U^+, followed by the $5f^36d^17s^1$ configuration (sextet I) at 3.73 kJ mol^{-1}, the $5f^47s^1$ configuration (sextet II) at 58.85 kJ mol^{-1}, and the $5f^37s^2$ configuration (doublet) at 115.95 kJ mol^{-1}.[10]

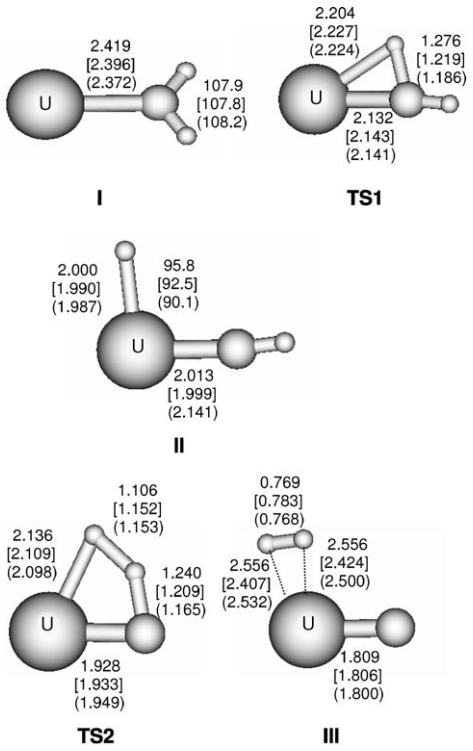

Figure 2. Geometrical parameters of minima and transition states at the B3LYP/SDD, PW91/SDD (in square brackets), and PW91/ZORA (in parentheses) levels for the reaction of U^+ (quartet state) with H_2O. Bond lengths are in Å and angles in deg.

the U^+ insertion into a O–H bond to form the $HUOH^+$ intermediate (**II**). The formation of this intermediate, which is a highly exothermic process, is possible after the system surpasses the first transition state (**TS1**). The reaction, then, can proceed toward the formation of the dehydrogenation products [Eq. (1)], through a concerted four-center elimination of H_2; or toward the formation of UOH^+, as the result of a simple cleavage of the U–H bond in the intermediate **II** [Eq. (2)]. The formation of the GS insertion complex is energetic enough so that the exit channel leading to the formation of the products could be kinetically reached. Activation barriers for all the TSs along the paths are reported in Table 1.

As can be seen in Figure 1, the second exit channel, namely the formation of UOH^+ (quintet state) with a loss of an H atom, is exothermic and has no barriers in excess of the reactant energy, in agreement with the ion-beam experiments.[6] The exothermicity of this process, however, is lower than that of the dehydrogenation reaction. These results agree with the experimental conclusion that the formation of UO^+ is thermodynamically favored.[5,6] The calculated exothermicity for the dehydrogenation reaction fairly agrees with the experimental estimation (about 315 kJ mol^{-1}).[7]

In addition to the previously mentioned dehydrogenation path, which involves the formation of the $(H_2)UO^+$ intermediate, we also considered the formation of a dihydride uranium oxo ion, $(H)_2UO^+$. However, in a quite large inspection of the potential energy surfaces, we could localize this species only for U^+ doublet states. In each case, the $(H)_2UO^+$ isomer has been found to be higher in energy than the $(H_2)UO^+$ isomer.

Table 1: Activation barriers [kJ mol^{-1}] of the transition states (see Figures 1 and 3).

U^+–H_2O	B3LYP/ SDD	PW91/ SDD	PW91/ ZORA	PW91/SO-ZORA
TS1[a]	60.76	34.48	17.95	21.97
TS2[b]	132.12	77.97	66.12	65.83
dissociation barrier[c]	73.03	36.37	47.71	41.10
U^{2+}–H_2O	B3LYP/ SDD	PW91/ SDD	PW91/ ZORA	PW91/SO-ZORA
TS1′[a]	143.41	128.73	112.83	110.40
TS2′[b]	124.67	106.13	108.22	69.93
dissociation barrier[c]	55.63	61.85	86.13	52.35

[a] Calculated as the energy difference between the first transition state and the first complex (**I** or **IV**). [b] Calculated as the energy difference between the second transition state and the first intermediate (**II** or **V**). [c] Energy difference between the dissociated products ($UO^+ + H_2$ or $UO^{2+} + H_2$) and the last intermediate (**III** or **VI**).

We have ensured that every transition state had only one imaginary frequency and, by performing IRC (intrinsic reaction coordinate) calculations, that this frequency connects reactants and products. Therefore we are confident that the dehydrogenation pathway involves the $(H_2)UO^+$ intermediate. Geometrical parameters of all the stationary points along the dehydrogenation path are presented in Figure 2. All the structures are planar, with the exception of $HUOH^+$, in which there is a deviation from planarity by about 4 deg.

An analysis analogous to that for the U^+ reaction revealed a similar reaction mechanism for the interaction between U^{2+} and H_2O. The high-spin/low-spin splittings for the bare U^{2+} cation at all the studied levels of theory are given in Figure 3,[10] which also shows the reaction profile for the reaction. The situation is quite different from that of the reaction of U^+. Firstly, there is a crossing of the potential energy surfaces just after the first transition state. After this point, the reaction evolves along the triplet-state surface. We were not able to characterize the second transition state for the quintet state, independent of the level of theory employed. However, this structure is surely quite high in energy and it is not fundamental for the description of the pathway, which evolves at this stage along the triplet-state surface.

A comparison between the reaction pathways (Figures 1 and 3) and the barrier heights (Table 1) indicates that the reaction of U^{2+} has to surpass a higher barrier for the first transition state (around 85 kJ mol^{-1} higher than in the reaction of U^+). The second barrier height (TS2) is comparable for both reactions, whereas the dissociation barrier is 17.4 kJ mol^{-1} higher than for the reaction of U^+.

Experimental studies led to partly contrasting results regarding the reaction products for the reaction of U^{2+} with H_2O. FTICR-MS results[9] indicated that the only reaction product is UOH^{2+}, whereas QIT-MS studies[5] detected both reaction products, that is, UOH^{2+} and UO^{2+}. From our

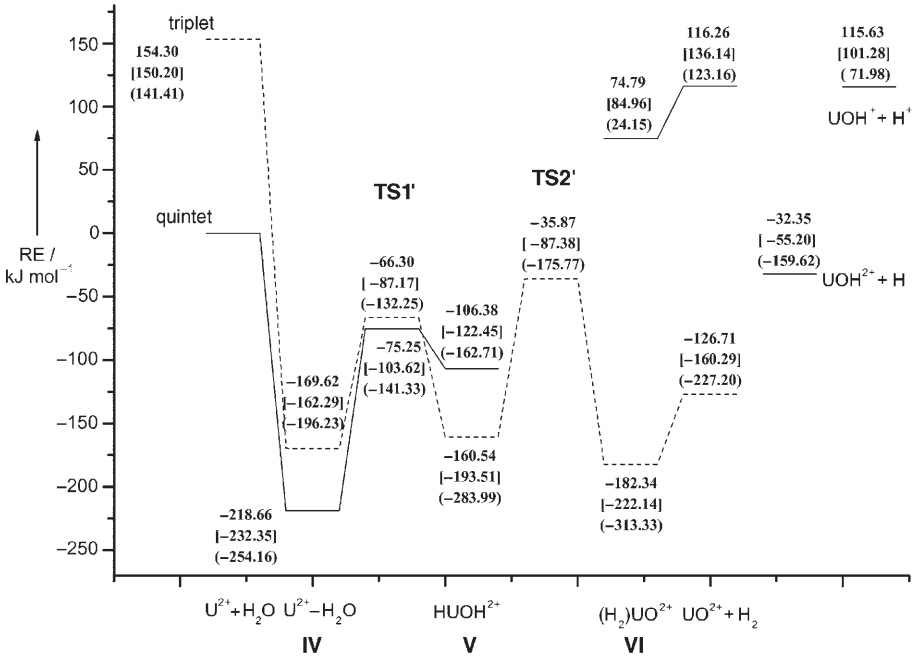

Figure 3. Potential energy profiles (RE: relative energy, in kJ mol^{-1}) for the reaction of U^{2+} with H_2O at the B3LYP/SDD, PW91/SDD (in square brackets), and PW91/ZORA (in parentheses) levels for the quintet (——) and triplet (-----) states of U^{2+}.[10] The lowest energy triplet state reported in the Blaise and Wyart tables[10] has the $5f^2 7s^2$ configuration and is 442 ± 72 kJ mol^{-1} higher in energy than the quintet GS. The $5f^4$ triplet state is not reported in these tables[10]. Our calculations indicated the $5f^4$ configuration to be the lowest-energy triplet state at 154.30 kJ mol^{-1}, whereas the $5f^2 7s^2$ triplet state is calculated to be at 419 kJ mol^{-1} from the quintet GS (B3LYP calculations).

theoretical results, we conclude that the thermodynamically favored reaction channel corresponds to the dehydrogenation process, whereas the products $UOH^{2+} + H$ have been found to be about 95 kJ mol^{-1} higher in energy (see Figure 3).

For the reaction of U^{2+}, we also considered the charge-separation asymptotes, that is, $UOH^+ + H^+$ and $UH^+ + OH^+$. The first one has been included in Figure 3. The $UH^+ + OH^+$ asymptote has been found to be much higher in energy; its endothermicity with respect to the $U^{2+} + H_2O$ asymptote was calculated to be 651.6 kJ mol^{-1} (B3LYP/SDD).

In Figure 4, we report the geometrical parameters for all the species involved in the reaction with U^{2+} (GS species). All the structures are planar, with the exception of the last insertion structure (**VI**), in which there is a deviation from planarity of about 6 deg (H_2 fragment with respect to UO).

Bonding was studied by means of natural bond orbital (NBO) and natural population analyses (NPA). The main conclusions obtained from these analyses can be summarized as follows. NPA analyses indicate that all the species involved in the reaction path have a highly ionic character, mainly from **TS1**/**TS1**′ to the products. This feature is particularly noticeable in the case of U^+, for which the charge on the metal center becomes +2.32 for $HUOH^+$. It is interesting to note, that the electronic configuration and the charge on the metal center corresponding to the same reaction species on the reaction paths of U^+ and U^{2+} seem to be quite close (e.g., NPA charge of U in $HUOH^+$: 2.32; of U in $HUOH^{2+}$: 2.87), which indicates more electron transfer from the metal center to the ligand in the case of U^+.

A detailed description of the NBO analysis is available as Supporting Information, which also offers some insight into the bonding evolution along the reaction paths and the direct role of 5f uranium electrons.

In summary, a DFT study of the reactions of U^+ and U^{2+} with H_2O had the following results: 1) for both reactions the dehydrogenation process is thermodynamically favored; 2) the exothermic formation of H_2 in the reaction between U^+ and H_2O takes place without changes in the spin state of the system; 3) the reaction of U^{2+} with water is less favored, both thermodynamically and kinetically, and involves a spin transition between a quintet and a triplet state; 4) no sharp differences between the theoretical approaches employed in this work have been found, which could permit us to decide which of them is the better one. The B3LYP functional seems to better reproduce the experimental data of bare uranium cations, whereas the PW91 functional shows a better agreement with experimental estimations of thermochemical data. The

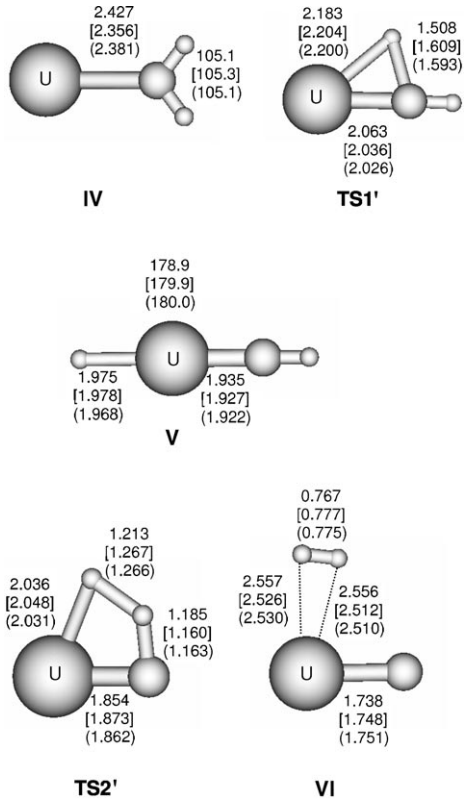

Figure 4. Geometrical parameters of minima and transition states at the B3LYP/SDD, PW91/SDD (in square brackets), and PW91/ZORA (in parentheses) levels for the reaction of U^{2+} with H_2O. Bond lengths are in Å and angles in deg.

inclusion of spin–orbit corrections generally decreases the activation barriers by 1 to 38 kJ mol^{-1}.

Received: June 3, 2005
Revised: October 31, 2005
Published online: January 3, 2006

Keywords: actinides · density functional calculations · gas-phase chemistry · O–H activation

[1] a) P. B. Armentrout, *Annu. Rev. Phys. Chem.* **1990**, *41*, 313 – 344; b) K. Eller, H. Schwarz, *Chem. Rev.* **1991**, *91*, 1121 – 1177; c) J. C. Weisshaar, *Acc. Chem. Res.* **1993**, *26*, 213 – 219.
[2] C. Heinemann, H. H. Cornehl, H. Schwarz, *J. Org. Chem.* **1995**, *60*, 201 – 209.
[3] J. K. Gibson, *Int. J. Mass Spectrom.* **2002**, *214*, 1 – 21.
[4] B. Liang, R. D. Hunt, G. P. Kushto, L. Andrews, *Inorg. Chem.* **2005**, *44*, 2159 – 2168.
[5] G. P. Jackson, F. L. King, D. E. Goeringer, D. C. Duckworth, *J. Phys. Chem. A* **2002**, *106*, 7788 – 7794.
[6] P. B. Armentrout, J. L. Beauchamp, *Chem. Phys.* **1980**, *50*, 27 – 36.
[7] H. H. Cornehl, R. Wesendrup, M. Diefenbach, H. Schwarz, *Chem. Eur. J.* **1997**, *3*, 1083 – 1090.
[8] M. Santos, J. Marçalo, A. Pires de Matos, J. K. Gibson, R. G. Haire, *J. Phys. Chem. A* **2002**, *106*, 7190 – 7194.
[9] J. K. Gibson, R. G. Haire, M. Santos, J. Marçalo, A. Pires de Matos, *J. Phys. Chem. A* **2005**, *109*, 2768 – 2781.
[10] The calculated first and second adiabatic ionization energies (IE1, IE2; in eV) for a U atom are: B3LYP/SDD: 6.42, 11.58; PW91/SDD: 5.56, 11.18; PW91/ZORA: 5.91, 11.13; the experimental values are: IE1:6.19, IE2:11.59. The experimental energy levels and ionization energies have been taken from J. Blaise, J.-F. Wyart, *International Tables of Selected Constants, Energy Levels and Atomic Spectra of Actinides, Vol. 20*, Tables of Constants and Numerical Data, Paris, **1992**. The calculated relative energies for the lowest-energy PW91/SO-ZORA configurations (*jj* coupling) are: for U^+: $5f^3_{5/2}7s^2_{1/2}$ as GS, $5f^4_{5/2}7s^1_{1/2}$ at +36.76 kJ mol^{-1}, $5f^2_{5/2}5f^1_{7/2}7s^2_{1/2}$ at +65.27 kJ mol^{-1}, and $5f^3_{5/2}6d^1_{3/2}7s^1_{1/2}$ at +75.02 kJ mol^{-1}; for U^{2+}: $5f^4_{5/2}$ as GS and $5f^3_{5/2}5f^1_{7/2}$ at +58.72 kJ mol^{-1}. The calculated total energies (in atomic units) of the GS cations at the different levels of theory are: B3LYP/SDD: $U^+ = -476.6219577$, $U^{2+} = -476.19053$; PW91/SDD: U^+:−476.7041557, $U^{2+} = -476.2747229$; in the case of PW91/ZORA, the values ($U^+ = 0.14066495$, $U^{2+} = 0.57073732$) correspond to relative energies with respect to the fragments, as implemented in the ADF package.

